AIP Applied Physics Letters

The effect of trimethylgallium flows in the AlInGaN barrier on optoelectronic characteristics of near ultraviolet light-emitting diodes grown by atmospheric pressure metalorganic vapor phase epitaxy

Yi-Keng Fu, Ren-Hao Jiang, Yu-Hsuan Lu, Bo-Chun Chen, Rong Xuan, Yen-Hsiang Fang, Chia-Feng Lin, Yan-Kuin Su, and Jenn-Fang Chen

Citation: Applied Physics Letters **98**, 121115 (2011); doi: 10.1063/1.3571440
View online: http://dx.doi.org/10.1063/1.3571440
View Table of Contents: http://scitation.aip.org/content/aip/journal/apl/98/12?ver=pdfcov
Published by the AIP Publishing

Articles you may be interested in
Nitrogen-polar core-shell GaN light-emitting diodes grown by selective area metalorganic vapor phase epitaxy
Appl. Phys. Lett. **101**, 032103 (2012); 10.1063/1.4737395

Improvement of efficiency of GaN-based polarization-doped light-emitting diodes grown by metalorganic chemical vapor deposition
Appl. Phys. Lett. **98**, 241111 (2011); 10.1063/1.3601469

Improved luminescence properties of Eu-doped GaN light-emitting diodes grown by atmospheric-pressure organometallic vapor phase epitaxy
Appl. Phys. Lett. **97**, 051113 (2010); 10.1063/1.3478011

Near-ultraviolet light emitting diodes using strained ultrathin InN/GaN quantum well grown by metal organic vapor phase epitaxy
Appl. Phys. Lett. **96**, 101115 (2010); 10.1063/1.3360199

Comparison of blue and green In Ga N Ga N multiple-quantum-well light-emitting diodes grown by metalorganic vapor phase epitaxy
Appl. Phys. Lett. **86**, 101903 (2005); 10.1063/1.1866634

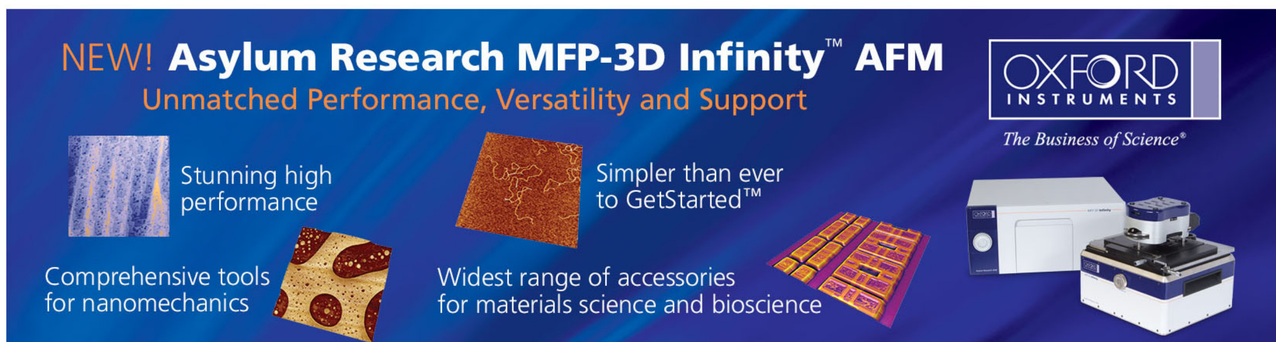

This article is copyrighted as indicated in the article. Reuse of AIP content is subject to the terms at: http://scitation.aip.org/termsconditions. Downloaded to IP: 140.113.38.11 On: Wed, 30 Apr 2014 09:14:18

The effect of trimethylgallium flows in the AlInGaN barrier on optoelectronic characteristics of near ultraviolet light-emitting diodes grown by atmospheric pressure metalorganic vapor phase epitaxy

Yi-Keng Fu,[1,a)] Ren-Hao Jiang,[1,2] Yu-Hsuan Lu,[1,3] Bo-Chun Chen,[1] Rong Xuan,[1,4] Yen-Hsiang Fang,[1] Chia-Feng Lin,[2] Yan-Kuin Su,[3] and Jenn-Fang Chen[4]
[1]*Electronics and Optoelectronics Research Laboratories, Industrial Technology Research Institute, Hsinchu 31040, Taiwan*
[2]*The Department of Materials Science and Engineering, National Chung Hsing University, Taichung 40227, Taiwan*
[3]*Department of Electrical Engineering, Institute of Microelectronics, National Cheng Kung University, Tainan 70101, Taiwan*
[4]*Department of Electrophysics, National Chiao Tung University, Hsinchu 30010, Taiwan*

(Received 14 December 2010; accepted 6 March 2011; published online 24 March 2011)

The letter reports a theoretical and experimental study on the device performance of near ultraviolet light-emitting diodes (LEDs) with quaternary AlInGaN quantum barrier (QB). The indium mole fraction of AlInGaN QB could be enhanced as we increased the trimethylgallium flow rate. It was found the AlInGaN/InGaN LEDs can reduce forward voltage and improve light output power, compared with conventional GaN QB. By using advanced device simulation, it should be attributed to a reduction in lattice mismatch induced polarization mismatch in the active layer, which results in the suppression of electron overflow. © *2011 American Institute of Physics*.
[doi:10.1063/1.3571440]

Recently, tremendous progress has been achieved in GaN-based blue, green, and ultraviolet light emitting diodes (LEDs).[1,2] Near ultraviolet (NUV) LEDs operating 400 nm wavelength is of special interest for solid-state lighting.[3] To achieve a shorter wavelength LED, one needs to reduce the indium (In) composition in the well layers so as to increase its band gap energy. However, since the quantum well (QW) In content of NUV LEDs is only a few percent the band offset between QW and (In)GaN quantum barrier (QB) becomes very small leading to poor carrier confinement and low efficiency. Replacing the (In)GaN barriers by AlGaN barriers significantly increases the band offset between QWs and barriers resulting in an increased efficiency.[4] However, the large lattice mismatch between AlGaN barrier and InGaN QW can result in the generation of defects at the AlGaN/InGaN interfaces as reported in Ref. 5. Another important aspect is the effect of the lattice mismatch and the strain between QB and QW on the piezoelectric polarization and the optical properties of the InGaN multiquantum well (MQW) active region. AlInGaN layers can be grown lattice matched to InGaN QW, which, in turn, can lead to a reduction in the piezoelectric polarization in the QW (Ref. 4) and interface defect.[5] However, to date, the optoelectronic characteristics of AlInGaN/InGaN MQW are quiet limited partially due to the difficult growth of these heterostructures with device quality.

Recently, Liu *et al.*[6] have been reported the In composition of AlInGaN epilayers increased with increasing growth rate and had good crystalline quality, which doesn't degrade with increasing growth rate. However, it is not clear the detailed results about AlInGaN/InGaN LEDs with various trimethylgallium (TMGa) flows. In this letter, we investigated the effect of AlInGaN barrier layers with various TMGa flows on InGaN LEDs grown by atmospheric pressure metalorganic vapor phase epitaxy (AP-MOVPE). The optoelectronic characteristics of AlInGaN/InGaN NUV LEDs will be demonstrated.

Samples used in this letter were all grown on c-face (0001) 2 in. sapphire (Al_2O_3) substrates in a SR-4000 AP-MOVPE. Prior to the growth, we heated the substrate to 1100 °C in H_2 ambient to remove surface contamination. We then deposited a 20-nm-thick low-temperature GaN nucleation layer at 500 °C. After the growth of GaN buffer layers, the temperature was then raised to 1110 °C to grow a 4-μm-thick undoped GaN epitaxial layer with a growth rate of 3.2 μm/h. The 300-nm-thick quaternary AlInGaN layer was subsequently grown on the undoped GaN template at 790 °C for 1 h using N_2 as the carrier gas. During the growth of AlInGaN layer, we kept the flow rates of trimethylaluminum (TMAl), trimethylindium, and ammonia (NH_3) at 0.4 μmol/min, 14.0 μmol/min, and 0.4 mol/min. On the other hand, the TMGa flow rate was kept at 10.4 μmol/min, 20.7 μmol/min, 31.1 μmol/min, and 41.4 μmol/min for samples I, II, III, and IV, respectively. We also prepared the AlGaN layer that the TMAl, TMGa, and NH_3 were introduced, labeled as sample V.

Nitride-based LEDs were then fabricated using these various QB layers. LED structure consists of a 20-nm-thick LT GaN nucleation layer, a 4-μm-thick Si-doped GaN *n*-cladding layer, an MQW active layer and a 200-nm-thick Mg-doped GaN layer. The MQW active region consists of five periods of 2.4-nm-thick undoped $In_{0.09}Ga_{0.91}N$ well layer and 9-nm-thick undoped AlInGaN barrier layer. We prepared LEDs I, II, and III with the AlInGaN QB grown with an TMGa flow of 10.4 μmol/min, 31.1 μmol/min, and 41.4 μmol/min, respectively. For comparison, conventional LED with GaN QB was also prepared, labeled as sample IV.

[a)]Author to whom correspondence should be addressed. Electronic mail: ykfu@itri.org.tw. Tel.:+886-3-5916951. FAX:+886-3-5915138.

 © 2011 American Institute of Physics
This article is copyrighted as indicated in the article. Reuse of AIP content is subject to the terms at: http://scitation.aip.org/termsconditions. Downloaded to IP: 140.113.38.11 On: Wed, 30 Apr 2014 09:14:18

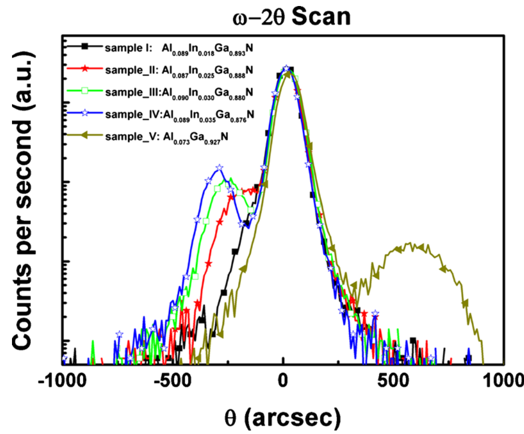

FIG. 1. (Color online) $\omega/2\theta$ scan spectra of AlInGaN-GaN heterostructure in the (0004) reflection.

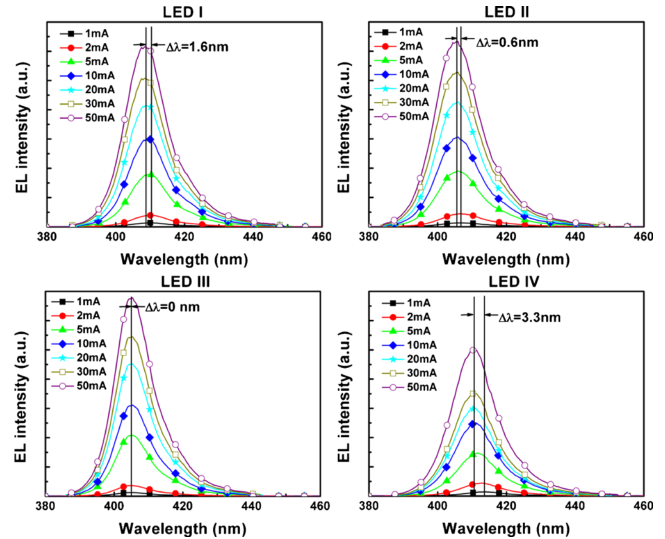

FIG. 2. (Color online) EL spectra of these three AlInGaN/InGaN LEDs and reference GaN/InGaN LED at various current injection levels.

For the fabrication of LEDs, we partially etched the surface of the samples until the *n*-type GaN layers were exposed. LEDs with indium tin oxide serving as a transparent contact layer were fabricated. We subsequently deposited Cr/Au onto the exposed *n*-type GaN layer to serve as the *n*-type electrode. The chip size of LEDs was 375 μm $\times$ 375 μm. High-resolution double-crystal x-ray diffractometer was performed to characterize the crystal quality on the Bede D1 system. The x-ray photoelectron spectroscopy (XPS) was also used to determine the amount of aluminum and In incorporations. Current-voltage (I-V) characteristics of the fabricated devices were then measured at room temperature by an HP4156 semiconductor parameter analyzer. The output powers were measured using the molded LEDs with the integrated sphere detector.

Figure 1 shows (0004) triple-axis $\omega/2\theta$ x-ray diffraction patterns for these five samples with different TMGa flow rates. The center peaks at 0 arc sec originate from the underlying GaN layers. For sample V without any In incorporation, the aluminum composition was calculated by 8%. The AlInGaN peak and GaN peak were overlapped together for sample I. It indicated that lattice constant of AlInGaN layer matched perfectly with the underlying GaN layer. We can also observe clearly that the position of the AlInGaN related peak shifted toward left side as we increased the TMGa flow rate. It should be attributed to the increased lattice constant for the AlInGaN with high In content. On the other hand, the lattice mismatch between QW and QB could be reduced with increasing the TMGa flow rate. By XPS measurement, the In content in the AlInGaN layers increased from 1.8% to 3.5% as we increased the TMGa flow rate from 10.4 to 41.4 μmol/min. The evaporation of In species from the surface seems to be suppressed not only at lower temperature[7] but also at higher growth rates,[8] as the In species become "trapped" by the growing layer.

Figure 2 plots the electroluminescence (EL) spectra of these four LEDs at various current injection levels. With 20 mA current injection, it was found that room temperature EL peaks were 409 nm, 406 nm, 405 nm, and 411 nm, respectively. The blueshift wavelength in EL spectra was observed when AlInGaN QB was used in place of GaN QB. In addition, as the current is increased from 1 to 50 mA, the peak wavelength for the reference LED IV shifts by 3.3 nm; the peak wavelength for the LED I shifts by 1.6 nm. Moreover, the blueshift in the peak wavelength with increasing current is reduced when the In mole fraction in the AlInGaN QB increases. The peak wavelength of LED III is almost independent of the driving current. Typically, strong blueshifts with increasing injection current are observed for QW structure with large piezoelectric field due to the quantum confined Stark effect and the screening of the piezoelectric fields with increasing carrier density.[9] Therefore, the different shifts in the peak wavelength are more likely related to the different spontaneous polarizations in InGaN QWs. It was attributed to a further reduction in the sheet charge magnitude by increasing In incorporation of AlInGaN QB.

Light-current-voltgae (L-I-V) characteristics of these four fabricated LEDs are also plotted in Fig. 3. With 20 mA current injection, it was found that forward voltages were 3.17 V, 3.14 V, 3.09 V, and 3.23 V for LEDs I, II, III, and IV, respectively. Recently, Kuo *et al.*.[10] have been reported the lattice mismatch and corresponding interface charge densities are reduced when the GaN QB are replaced by the $In_{0.02}Ga_{0.98}N$ or $In_{0.05}Ga_{0.95}N$ QB. The conduction band on the *n*-side of the device is approximately the same height as the conduction band on the *p*-side, which indicates that the polarization-matched active region design minimizes the device force for electrons to leak out of the active region. In this letter, the lattice mismatch between QW and QB and corresponding interface charge densities are reduced by increasing In incorporation of AlInGaN QB, which is benefi-

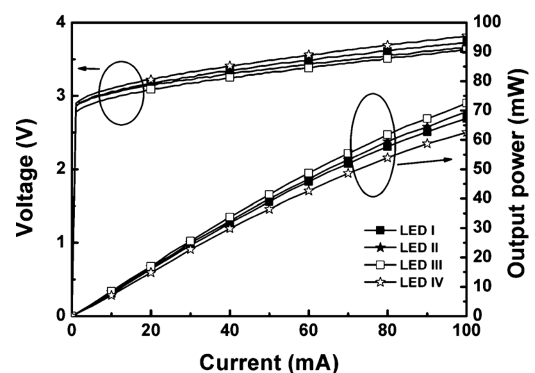

FIG. 3. L-I-V characteristics of these four fabricated LEDs.

This article is copyrighted as indicated in the article. Reuse of AIP content is subject to the terms at: http://scitation.aip.org/termsconditions. Downloaded to IP: 140.113.38.11 On: Wed, 30 Apr 2014 09:14:18

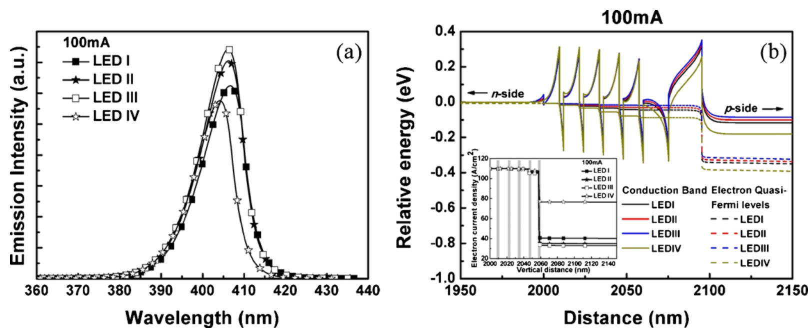

FIG. 4. (Color online) (a) The calculated EL spectra and (b) conduction band diagram of these four LEDs at 100 mA current injection. The inset of Fig. 4(b) shows the vertical electron current density profiles near the active regions.

cial for reducing the forward voltage. It was also found that output power of LEDs with AlInGaN QB was larger than that of LED with GaN QB under the same current injection. Under 100 mA current injection, the LED I output power can be enhanced by 7.6% by using AlInGaN QB, compared with LED IV. The slightly larger output power observed from LED I can be attributed to a reduction in lattice constant induced polarization mismatch in the active $In_{0.09}Ga_{0.91}N$ layer. The output power of AlInGaN/InGaN LEDs could be more enhanced as we increased the TMGa flow rate. It was also attributed to the reduced lattice mismatch between QW and QB by increasing In incorporation of AlInGaN QB.

In order to investigate the physical mechanisms responsible for the improvement of light output power, numerical simulations of these LED structures with various AlInGaN QBs are performed using the Simulator of Light Emitters based on Nitride Semiconductors (SILENSE) 4.2 software, developed by the STR Crop.[11] The simulated structures, such a layer thicknesses, doping concentrations, Al and In composition are the same as the actual devices and the corresponding nitride materials parameters are used in the calculations. Figure 4(a) shows the calculated EL spectra of these four LEDs at a current injection of 100 mA. Compared with LED IV, the simulated EL intensity of LED III can be enhanced by 28.8%. Figure 4(b) shows the simulated conduction band diagram of these four LEDs at a 100 mA forward current. The conduction band on the *n*-side of the device is approximately the same height as the conduction band on the *p*-side, which indicates that the polarization-matched active region design minimizes the device force for electron to leak out of the active region. The inset of Fig. 4(b) shows the vertical electron current density profiles near the active regions of these four LEDs when the current injection is 100 mA. The positions of five QWs are marked with gray areas. The electron current is injected from *n*-type layers into QWs and recombines with holes. The electron current which overflows through QWs is viewed as leakage current. After using AlInGaN QBs, the electron overflow can be significantly decreased and the leakage current can be further suppressed by increasing the TMGa flow from 10.4 to 41.4 μmol/min. Therefore, the improvement of LED light output power could be attributed the fact that a reduction in lattice mismatch induced polarization mismatch in the active layer, which results in the suppression of electron overflow.

In summary, an $Al_{0.089}In_{0.018}Ga_{0.897}N$ quaternary layer which was lattice matched to GaN was successful grown. The In incorporation of AlInGaN layer increases with increasing TMGa flow rate. It was found the AlInGaN/InGaN LED can reduce forward voltage, reduced the shift in wavelength with increasing current and improved light output power by reducing the lattice mismatch induced the polarization mismatch and sheet charges between QW and QB, compared with conventional GaN QB. Under 100 mA current injection, the LED output power with $Al_{0.089}In_{0.035}Ga_{0.876}N$ QB can be enhanced by 15.9%, compared with LED with GaN QB. It could be attributed the fact that a reduction in lattice mismatch induced polarization mismatch in the active layer, which results in the suppression of electron overflow through theoretical simulation.

[1]T. Mukai, S. Nagahama, M. Sano, T. Yanamoto, D. Morita, T. Mitani, Y. Narukawa, S. Yamamoto, I. Niki, M. Yamada, S. Sonobe, S. Shioji, K. Deguchi, T. Nau, H. Tamaki, Y. Murazaki, and M. Kameshima, Phys. Status Solidi A **200**, 52 (2003).
[2]M. Yamada, T. Mitani, Y. Narukawa, S. Shioji, I. Niki, S. Sonobe, K. Deguchi, M. Sano, and T. Mukai, Jpn. J. Appl. Phys., Part 2 **41**, L1431 (2002).
[3]Y. Narukawa, I. Niki, K. Izuno, M. Yamada, Y. Murazki, and T. Mukai, Jpn. J. Appl. Phys., Part 2 **41**, L371 (2002).
[4]A. Knauer, V. Kueller, S. Einfeldt, V. Hoffmann, T. Kolbe, J. R. van Look, J. Piprek, M. Weyers, and M. Kneissl, Proc. SPIE **6797**, 67970X (2007).
[5]O. Goto, S. Tomiya, Y. Hoshina, T. Tanaka, M. Ohta, Y. Ohizumi, Y. Yabuki, K. Funato, and M. Ikeda, Proc. SPIE **6485**, 64850Z (2007).
[6]J. P. Liu, B. S. Zhang, M. Wu, D. B. Li, J. C. Zhang, R. Q. Jin, J. J. Zhu, J. Chen, J. F. Wang, Y. T. Wang, and H. Yang, J. Cryst. Growth **260**, 388 (2004).
[7]S. Keller, S. F. Chichibu, M. S. Minsky, E. Hu, U. K. Mishra, and S. P. DenBaars, J. Cryst. Growth **195**, 258 (1998).
[8]S. Keller, B. P. Keller, D. Kapolnek, U. K. Mishra, S. P. DenBaars, I. K. Shmagin, R. M. Kolbas, and S. Krishnankutty, J. Cryst. Growth **170**, 349 (1997).
[9]J. Li, S. L. Shi, Y. J. Wang, S. J. Xu, D. G. Zhao, J. J. Zhu, H. Yang, and F. Lu, IEEE Photon. Technol. Lett. **19**, 789 (2007).
[10]Y. K. Kuo, J. Y. Chang, M. C. Tsai, and S. H. Yen, Appl. Phys. Lett. **95**, 011116 (2009).
[11]SILENSE Physics Summary, http://www.semitech.us/products/SiLENSe/.

This article is copyrighted as indicated in the article. Reuse of AIP content is subject to the terms at: http://scitation.aip.org/termsconditions. Downloaded to IP: 140.113.38.11 On: Wed, 30 Apr 2014 09:14:18